Applied Physics A (2020) 126:312
https://doi.org/10.1007/s00339-020-03495-5

Applied Physics A
Materials Science & Processing

Determination of carrier lifetime in thermally evaporated In_2S_3 thin films by light induced transient grating technique

S. Rasool[1] · P. Ščajev[3] · K. Saritha[1] · I. Svito[2] · K. T. Ramakrishna Reddy[1] · M. S. Tivanov[2] · V. Grivickas[3]

Received: 29 November 2019 / Accepted: 23 March 2020

Abstract
In_2S_3 thin films were deposited onto soda lime glass substrates using thermal evaporation technique at a constant substrate temperature of 300 °C and the films were annealed in a sulfur ambient at 250 °C and 300 °C for 1 h. Light induced transient grating (LITG) technique was used to determine the carrier lifetime in In_2S_3 thin films. The determined carrier lifetime values for different excitation energy densities, $I_0 = 0.06–1.64$ mJ/cm^2 decreased from 206 to 18 ps and 150 to 14 ps for the films annealed at 250 °C and 300 °C respectively. Further, the bimolecular, Auger recombination coefficients and diffusion coefficient were determined in the films. The observed bimolecular carrier recombination origin was explained by interface and Auger recombination processes.

Keywords In_2S_3 films · LITG · Carrier lifetime · Bimolecular coefficient · Auger coefficient

1 Introduction

Cu(In,Ga)Se_2 (CIGSe) and CdTe-based solar cells have reached high conversion efficiencies of 22.6% and 22.1% using CdS as a buffer layer [1, 2] and are currently commercialized. But, the large scale production of these solar cells using CdS is environmentally unsafe to handle because of the toxicity of cadmium. Therefore, alternate materials are of much interest now that can successfully replace CdS. In this context, In_2S_3 is a potential alternative material, because of its wide energy band gap (2.0–3.3 eV), n-type conductivity, non-toxic and photoconductive nature [3–6]. Recently, Spiering et al. [7] reported a record solar cell efficiency of 18.2% using evaporated In_2S_3 thin film as a buffer layer for Cu(In,Ga)Se_2-based thin film solar cells.

Charge carrier lifetime is one of the important parameters that significantly influence the performance of optoelectronic devices. Determination of carrier lifetime and carrier diffusion length of the material is highly essential before fabrication of any device. Generally, carrier lifetime is sensitive to impurities or defects that are present in the material. In direct band gap semiconductors, the lifetime of charge carriers is of the order of nanoseconds to microseconds, depending upon the excess carrier concentration and defect properties. The measurement of carrier lifetime is based on the dynamics of excess photo-generated charge carriers. Various techniques such as time-resolved photoluminescence spectroscopy (TRPL) [8], transient absorption spectroscopy (TAS) [9–11], time-resolved terahertz spectroscopy (TRTS) [12], time-resolved microwave conductivity (TRMC) [13–15], steady-state photo-carrier grating (SSPG) [16] and light-induced transient grating (LITG) [17–19] have been used to measure the carrier dynamics in semiconductors. To the best of our knowledge, there are no such reports on the use of LITG technique to find the carrier lifetime and determine recombination mechanisms in In_2S_3 layers. Therefore, picosecond LITG technique was employed to measure the carrier lifetime (τ) and diffusion coefficient (D) in In_2S_3 thin films for the first time in the present work and the results are discussed.

✉ K. T. Ramakrishna Reddy
ktrkreddy@gmail.com

[1] Solar Photovoltaic Laboratory, Department of Physics, Sri Venkateswara University, Tirupati, Andhra Pradesh 517 502, India

[2] Faculty of Physics, Belarusian State University, Nezavisimosti 4 Av, 220030 Minsk, Belarus

[3] Institute of Photonics and Nanotechnology, Vilnius University, Sauletekio ave. 3, LT-10257 Vilnius, Lithuania

Published online: 01 April 2020

2 Experimental

In_2S_3 films of ~ 500 nm thickness were produced by thermal evaporation technique using 5 N pure In_2S_3 powder obtained from Sigma Aldrich company. The layers were formed on soda lime glass substrates at a temperature of 300 °C, followed by annealing in sulfur atmosphere at 250 °C and 300 °C for 1 h. The detailed deposition conditions of the films were reported elsewhere [20]. LITG is an optical pump–probe technique used to measure the photo induced τ and D parameters. In this technique, a Nd:YLF laser pump beam of 351 nm wavelength ($h\nu >$ bandgap energy, E_g of the sample) was split into two laser pulses (pulse duration of 10 ps) that interfere at the sample. As a result, a periodically modulated excess carrier density N(x) was generated. The latter acts as a transient diffraction grating in the sample. In order to monitor the carrier dynamics, an optically delayed probe beam of 1053 nm wavelength was incident upon the sample. This probe beam gets transmitted through the sample and diffracted at the transient grating as shown in Fig. 1.

The carrier density distribution is described as,

$$N(x) = \Delta N(1 + \cos(2\pi x/(\Lambda)) \quad (1)$$

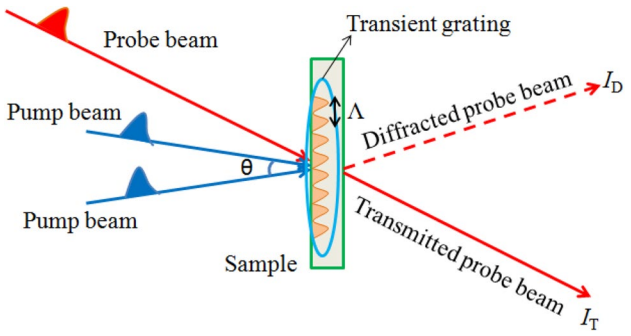

Fig. 1 Principle scheme of LITG technique

where $\Delta N = \alpha I_0/2\ h\nu$ (α is absorption coefficient, I_0 is the excitation energy density) and Λ is the transient grating period given by $\Lambda = \lambda/2\sin(\theta/2)$, where $\lambda = 351$ nm that is the wavelength of the pump beam and $\theta = 19.8°$, which is the angle between two pump beams respectively for $\Lambda = 3.2$ µm. The LITG diffraction efficiency (η) is defined as the ratio of diffracted beam intensity (I_D) to transmitted beam intensity (I_T) and is measured as a function of delay time between pump and probe pulses. Figure 2 shows the schematic representation of light-induced transient grating setup. The rate of diffusive grating erasure depends on Λ, while recombination rate does not, which allows to distinguish these two processes. The ambipolar τ and D parameters can be determined from LITG transients recorded for few different Λ, according to a relation: $1/\tau_G = 1/\tau + 4\pi^2 D/\Lambda^2$. Diffraction efficiency is described by a relation, DE ~ $\exp(-2t/\tau_G)$.

3 Results and discussion

Figure 3a and b show the LITG diffraction efficiency decay curves for In_2S_3 layers annealed at 250 °C and 300 °C for different grating periods, 0.73 µm, 1.6 µm and 3.2 µm. These plots provided the decay curves with different decay rates. While Fig. 3c and d show the decay curves of In_2S_3 layers for a grating period of 3.2 µm with different excitation energy densities (I_0) that varied in the range of 0.06–1.64 mJ/cm^2. The obtained decay patterns are non-exponential due to injection conditions. From these plots, the τ and D parameters can be directly obtained by fitting the decay pattern by exponents.

The determined carrier lifetime values for different excitation energy densities, $I_0 = 0.06$–1.64 mJ/cm^2 decreased from 206 to 18 ps and 150 to 14 ps for the films annealed at 250 °C and 300 °C respectively. Here, the decrease in carrier lifetime with increase of excitation energy density might be due to bimolecular, Auger or surface/interface recombination processes that occur in these films. Bondarenko et al. [21] also observed a similar decrease of carrier lifetime with

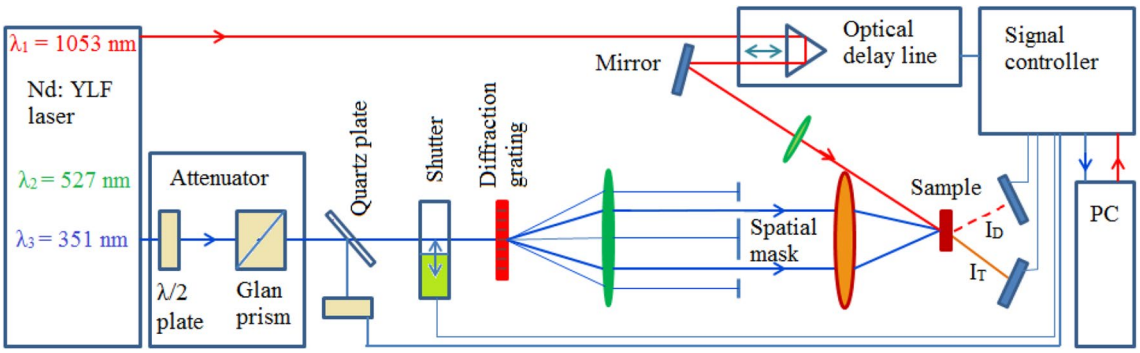

Fig. 2 Schematic representation of picosecond light-induced transient grating setup

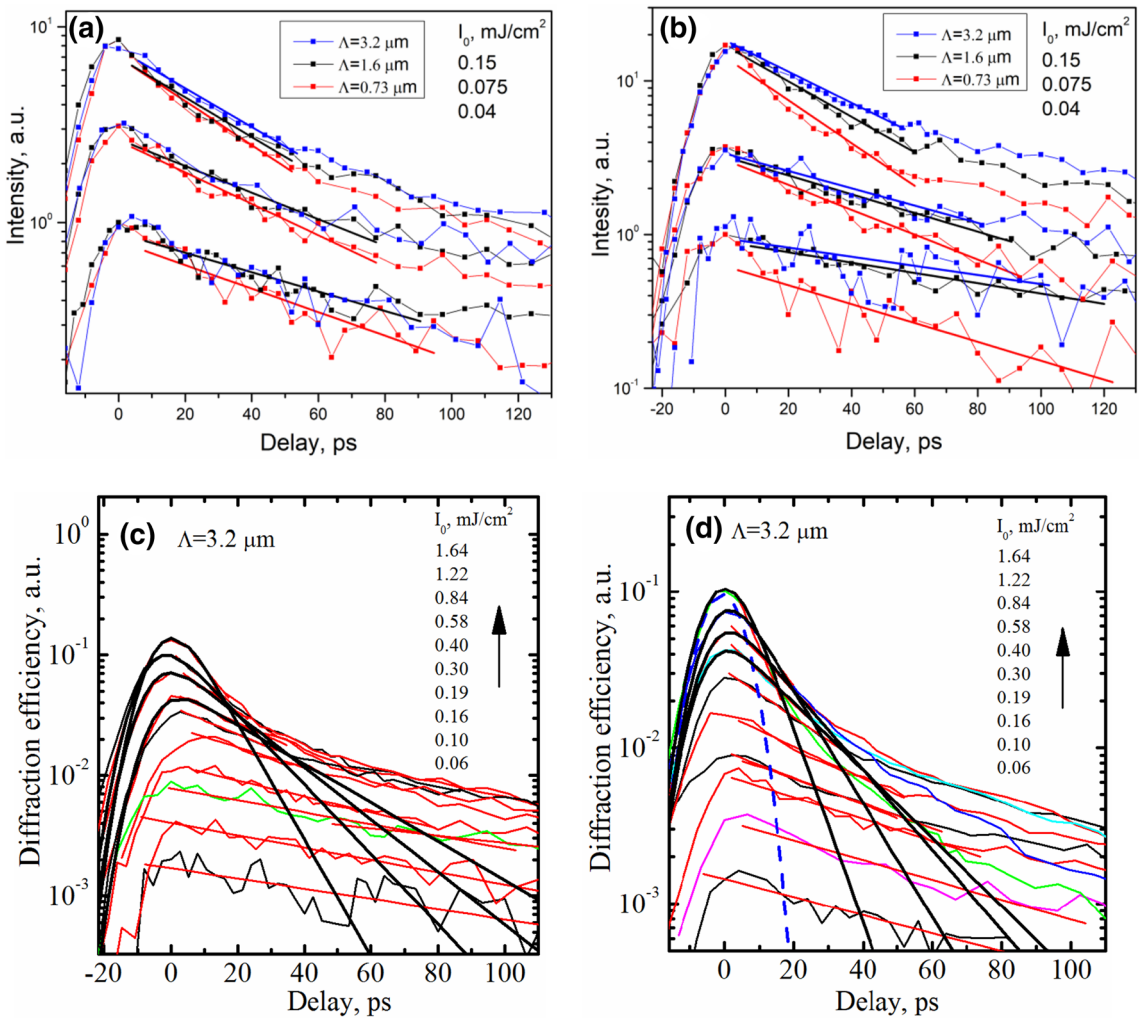

Fig. 3 LITG kinetics measured at different grating periods for In_2S_3 films annealed at **a** $T_a = 250$ °C and **b** $T_a = 300$ °C; solid lines are fits of the LITG grating decay time. The decay curves measured at a grating period of 3.2 μm with different excitation energy densities for In_2S_3 films annealed at **c** $T_a = 250$ °C and **d** $T_a = 300$ °C (Straight lines are exponential fits to the kinetics; laser response funtion of measurement system is shown by dashed line; solid curves show fitting of the initial decay parts by Erf fuction)

increase of excitation energy density for bismuth oxysulfide semiconductor films prepared by chemical bath deposition.

Figure 4 shows the variation of D with different excitation, from which, a low D value of 0.2–0.5 ± 0.1 cm^2/s was obtained due to cumulative effect of large hole mass [22] and carrier transport blocking by grain boundaries. Here, the observed increase of diffusivity with excitation can be related to carrier degeneracy.

Figure 5 shows the variation of carrier lifetime with excitation energy density of In_2S_3 films. As the highest excitation lifetime becomes comparable to the duration of response function of measurement system (see Fig. 3 d) ($\exp(-t^2/2\sigma^2)$, where $\sigma = 6$ ps), therefore deconvolution of the decay initial part was performed with Erf function [23], $DE(t) \sim \exp[(\sigma^2 - 2t\tau_e)/(2\tau_e^2)] \times [1 + \mathrm{Erf}\{(t\tau_e - \sigma^2)/(2^{1/2}\sigma\tau_e)\}]$, $\tau_G = 2\tau_e$, where τ_e is the exponential fit lifetime to the DE decay. The carrier lifetimes of the films were fitted well with bimolecular law, where the long term lifetime (τ_G) in the kinetic tails for the films annealed at 250 °C is 330 ps and is 240 ps for the layers annealed at 300 °C. The bimolecular fit was done for In_2S_3 films by the following relation (2), where the coefficient b value (0.027 and 0.032 $cm^2ps^{-1}mJ^{-1}$ for films annealed at 250 °C and 300 °C, respectively) can be directly obtained from the slope of the linear plot of τ^{-1} versus I_0 (not shown).

$$\tau = \left[\frac{1}{\tau_G} + bI_0\right]^{-1} \quad (2)$$

Figure 6 shows the dependence of carrier recombination lifetime on the non-equilibrium carrier density and interplaying recombination mechanisms (Interface and

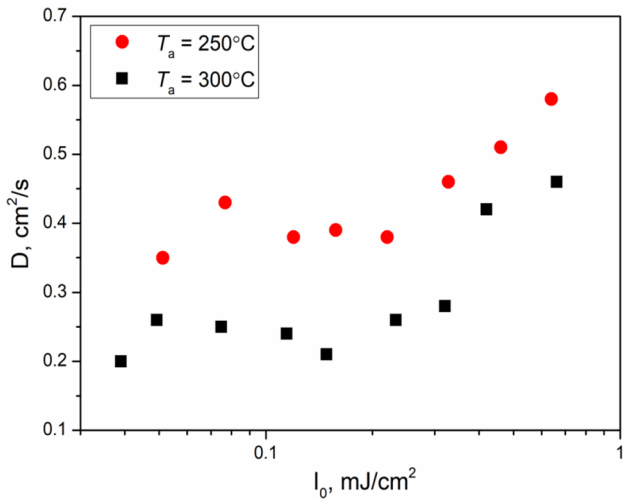

Fig. 4 Variation of the carrier diffusion coefficient with excitation energy density

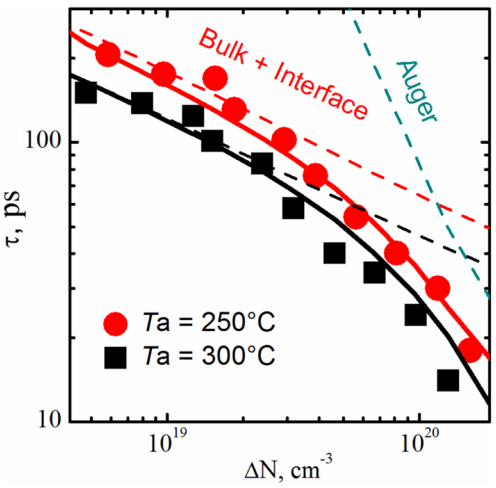

Fig. 6 Dependence of carrier recombination lifetime on non-equilibrium carrier density in In_2S_3 films. (Solid line shows fit including bulk, interface and Auger recombination mechanisms)

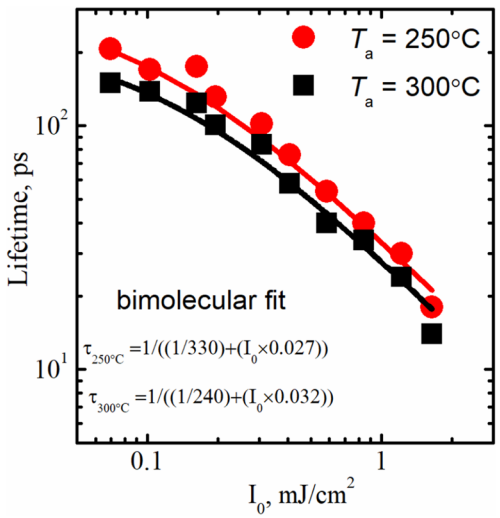

Fig. 5 Variation of the carrier lifetime with excitation energy density

Auger recombination) in In_2S_3 films. In general, the in-depth photogenerated carrier concentration (ΔN) is proportional to the excitation fluence when absorption depth ($1/\alpha$) is smaller than film thickness [24]

$$\Delta N = \alpha I_0 / 2h\nu. \tag{3}$$

Here, α is absorption coeffcient at 351 nm wavelength of pump beam, which was determined from conventional optical absorption spectroscopy and its values are 1.1×10^5 cm^{-1} and 0.9×10^5 cm^{-1} for the films annealed at 250 °C and 300 °C, respectively. The obtained ΔN values varied in the range, 5.8×10^{18} cm^{-3}–1.6×10^{20} cm^{-3} and 4.8×10^{18} cm^{-3}–1.3×10^{20} cm^{-3} for films annealed at 250 °C and 300 °C with respect to I_0.

The recombination rate is one of the limiting parameters of solar cell efficiency and depends on many parameters such as charge carrier mobility, carrier density and doping levels. The recombination rate ($1/\tau$) is proportional to the carrier concentration which is expressed as

$$\frac{1}{\tau(N)} = A + BN + CN^2 \tag{4}$$

where A, B and C describe the coefficients of linear, bimolecular (radiative) and Auger recombinations respectively. When C term is neglected in relation (4), the bimolecular coefficient, B ($= 2bh\nu/\alpha$) values were determined as ~ 3.3×10^{-10} cm^3/s and 3.2×10^{-10} cm^3/s for films annealed at $T_a = 250$ °C and 300 °C, respectively. Such values are similar to radiative recombination coefficient evaluated for different direct bandgap semiconductors, where values of 10^{-8}–10^{-11} cm^3/s are typical [25]. However, we observe only very weak photoluminescence (quantum efficiency was below 1% as checked by integrating sphere), therefore the determined B should reflect nonradiative processes.

Generally, trap-assisted recombination on the outer sides of any semiconductor sample is one of the current transport mechanisms that can influence the perfomance of the device, particularly the solar cells. As the layers grown in this work are rather thick (~ 500 nm) and diffusion coefficient is small ($D = 0.2$–0.5 cm^2/s), its prominence can be neglected. However, interface recombination at grain boundaries is the common recombination path that is observed in polycrystalline thin films [26–28]. The

Coulomb potential by defect charges at the grain boundaries of In_2S_3 films can be described by free carrier screening, which is mainly due to interface recombination. This interface recombination velocity (S_{int}) can be evaluated by the following relation [29],

$$S_{int}(\Delta N) = S_0\left(1 + 2\Delta N/n_0\right)^{1/2} \quad (5)$$

where, S_0 we fitted as 0.8 cm/s and 2.5 cm/s; n_0 is the equilibrium doping density, 3.6×10^{11} cm^{-3} and 17.5×10^{11} cm^{-3} in In_2S_3 films annealed at 250 °C and 300 °C respectively. The equilibrium doping density of the films was estimated from the carrier mobility, 16 cm^2/Vs and 4 cm^2/Vs for films annealed at 250 °C and 300 °C [30] and respective resistivity of these samples are 1.06×10^6 Ω•cm and 0.89×10^6 Ω•cm, determined using Ohmic contacts. The fitted S_{int} values (relation 5) in the LITG experiment increased from 3.1×10^5 to 16.3×10^5 cm/s and 1.2×10^5 to 6.7×10^5 cm/s with increase of ΔN in the layers. Anita Warrier et al. [31] determined similar values, which varied in the range, 5×10^3–11×10^3 cm/s in β-In_2S_3 films by using photothermal beam deflection technique. The interface related recombination lifetime (τ_i) is described by the following equation [32, 33],

$$\tau_i = \frac{r_{eff}}{1.77S_{int}} + \left(\frac{r_{eff}}{2.36}\right)^2 \frac{1}{D} \quad (6)$$

where r_{eff} is the average grain radius taken as 20 nm [20] and the D is taken to be > 0.2 cm^2/s. By setting these values in Eq. (6), the second term equals to < 4 ps, which indicates rather fast carrier transport to grain boundaries and thus first interface term should be limiting the recombination process. The evaluated values of τ_i varied in the range, 40–300 ps for the layers annealed at 250 °C and 300 °C. The recombination lifetime in In_2S_3 films at high carrier densities is controlled by Auger recombination and its coefficient C can be determined by fitting the lifetime excitation dependence with the following relation including bulk, interface and Auger recombination terms [33, 34],

$$\frac{1}{\tau} = \frac{1}{\tau_{bulk}} + \frac{1}{\tau_i} + C\left(\Delta N + n_0\right)\Delta N \quad (7)$$

The obtained C values are 0.8×10^{-30} cm^6/s and 1.5×10^{-30} cm^6/s and bulk lifetime (τ_{bulk}) values are 2000 ps and 1000 ps in the grains of In_2S_3 films annealed at 250 °C and 300 °C, respectively. The latter values are much larger than the interface recombination lifetime on grain boundaries. The Auger recombination rate decreased with increase of carrier density due to the Coulomb interaction [33, 35].

4 Conclusion

In_2S_3 thin films were thermally evaporated at 300 °C followed by annealing at 250 °C and 300 °C in sulfur ambient. The non-destructive light induced transient grating technique is used to determine the carrier lifetime in In_2S_3 films at different excitation energy densities. The films annealed at 250 °C showed better carrier lifetime values compared to those annealed at 300 °C. These values decreased with increase of excitation energy density and varied from 206 ps to 25 ps. The decrease of lifetime with the raise of excitation density is explained by recombination at the grain interfaces described by nonradiative bimolecular recombination, consisting of interface and Auger recombination processes. For films annealed at 250 °C, the evaluated bimolecular recombination coefficient is ~ 3×10^{-10} cm^3/s and the Auger recombination coefficient is 0.8×10^{-30} cm^6/s.

Acknowledgements One of the authors, S. Rasool is thankful to the University Grants Commission (UGC), New Delhi for the financial assistance via the "UGC-BSR fellowship". The authors, Prof. K.T. Ramakrishna Reddy and Prof. M.S. Tivanov wish to acknowledge the Dept. of Science and Technology, Govt. of India (Grant No: DST/INT/BLR/P-30/2019) and the State Committee on Science and Technology of the Republic of Belarus (Grant No: F19INDG-008). P. Ščajev acknowledges the financial support provided by the Research Council of Lithuania under the project No. S-MIP-19-34.

References

1. P. Jackson, R. Wuerz, D. Hariskos, E. Lotter, W. Witte, M. Powalla, Effects of heavy alkali elements in Cu(In, Ga) Se_2 solar cells with efficiencies up to 226%. Phys. Status Solidi RRL **10**, 583 (2016)
2. M.A. Green, K. Emery, Y. Hishikawa, W. Warta, E.D. Dunlop, Solar cell efficiency tables (version 48). Prog. Photovolt: Res. Appl. **24**, 905 (2016)
3. J. George, K.S. Joseph, B. Pradeep, T.I. Palson, Reactively evaporated films of indium sulfide. Phys. Status Solidi A **106**, 123 (1988)
4. E.B. Yousfi, B. Weiberg, F. Donsanti, P. Cowache, D. Lincot, Atomic layer deposition of zinc oxide and indium sulfide layers for Cu(In, Ga)Se2 thin-film solar cells. Thin Solid Films **387**, 29 (2001)
5. Y.J. Hsia, C.H. Lu, L.W. Ji, T.H. Meen, Y.L. Chen, H.P. Chi, Characterization of photovoltaics with In_2S_3 nanoflakes/p-Si heterojunction. Nanoscale Res. Lett. **9**, 32 (2014)
6. R. Yoosuf, M.K. Jayaraj, Optical and photoelectrical properties of β-In_2S_3 thin films prepared by two stage process. Sol. Energy Mater. Sol. Cells **89**, 85 (2005)
7. S. Spiering, A. Nowitzki, F. Kessier, M. Igalson, H.A. Maksoud, Optimization of buffer-window layer system for CIGS thin film devices with indium sulphide buffer by in-line evaporation. Sol. Energy Mater. Sol. Cells **144**, 544 (2016)
8. R.K. Ahrenkiel, Measurement of minority-carrier lifetime by time-resolved photoluminescence. Solid-State Electron. **35**, 239 (1992)

9. Z. Guo, J.S. Manser, Y. Wan, P.V. Kamat, L. Huang, Spatial and temporal imaging of long-range charge transport in perovskite thin films by ultrafast microscopy. Nat. Commun. **6**, 7471 (2015)
10. Z. Guo, Y. Wan, M. Yang, J. Snaider, K. Zhu, L. Huang, Long-range hot carrier transport in hybrid perovskite visualized by ultrafast microscopy. Science **356**, 59 (2017)
11. A.H. Hill, K.E. Smyser, C.L. Kennedy, E.S. Massaro, E.M. Grumstrup, Screened charge carrier transport in methylammonium lead iodide perovskite thin films. J. Phys. Chem. Lett. **8**, 948 (2017)
12. J.B. Baxter, C.A. Schmuttenmaer, Conductivity of ZnO nanowires, nanoparticles, and thin films using time-resolved terahertz spectroscopy. J. Phys. Chem. B. **110**, 25229 (2006)
13. R. Brenok, R. Vanderhaghen, B. Drevillon, I. French, R. i Cabarrocas, Time resolved microwave conductivity measurements for the characterization of transport properties in thin film microcrystalline silicon. Thin Solid Films **296**, 94 (1997)
14. J.G. Labram, M.L. Chabinyc, Recombination at high carrier density in methylammonium lead iodide studied using time-resolved microwave conductivity. J. Appl. Phys. **122**, 065501 (2017)
15. T.J. Savenije, M. Nanu, A time-resolved microwave conductivity study of the optoelectronic processes in $TiO_2/In_2S_3/CuInS_2$ heterojunctions. J. Appl. Phys. **101**, 113718 (2007)
16. M. Niehus, R. Schwarz, New results on diffusion lengths measurements in wide bandgap semiconductors, obtained from steady state photocarrier gratings (SSPG). Superlattices Microstruct. **40**, 350 (2006)
17. J. Mickevičius, M.S. Shur, R.S.Q. Fareed, J.P. Zhang, R. Gaska, G. Tamulaitis, Time-resolved experimental study of carrier lifetime in GaN epilayers. Appl. Phys. Lett. **87**, 241918 (2005)
18. D.H. Arias, D.T. Moore, J. Lagemaat, J.C. Johnson, Direct measurements of carrier transport in polycrystalline methyl ammonium lead iodide perovskite films with transient grating spectroscopy. J. Phys. Chem. Lett. **9**, 5710 (2018)
19. P. Ščajev, R. Aleksiejūnas, S. Miasojedovas, S. Nargelas, M. Inoue, C. Qin, T. Matsushima, C. Adachi, S. Juršėnas, Two regimes of carrier diffusion in vapor deposited lead-halide perovskites. J. Phys. Chem. C **121**, 21600 (2017)
20. S. Rasool, K. Saritha, K.T. Ramakrishna Reddy, M.S. Tivanov, A.V. Trofimova, S.E. Tikoto, L. Bychto, A. Patryn, M. Maliński, V.F. Gremenok, Effect of annealing on the physical properties of thermally evaporated In_2S_3 thin films. Cur Appl Phys **19**, 108 (2019)
21. E.A. Bondarenko, E.A. Streltsov, A.V. Mazanik, A.I. Kulak, V. Grivickas, P. Ščajev, E.V. Skorb, Bismuth oxysulfide film electrodes with giant incident photon-to-current conversion efficiency: dynamics of properties with deposition time. Phys. Chem. Chem. Phys. **20**, 20340 (2018)
22. Z. Zhao, Y. Cao, J. Yi, X. He, C. Ma, J. Qiu, Band-edge electronic structure of β-In2S3: the role of s or p orbitals of atoms at different lattice positions. Chem. Phys. Chem. **13**, 1551 (2012)
23. E.P. Farr, J.C. Quintana, V. Reynoso, J.D. Ruberry, W.R. Shin, K.R. Swartz, Introduction to Time-Resolved Spectroscopy: nanosecond Transient Absorption and Time-Resolved Fluorescence of Eosin B. J. Chem. Educ. **95**, 864 (2018)
24. P.B. Klein, R. Myers-Ward, K.K. Lew, B.L. Van Mil, C.R. Eddy, D.K. Gaskill, A. Shrivastava, T.S. Sudarshan, J. Appl. Phys. **108**, 033713 (2010)
25. M. Grundmann, *The Physics of Semiconductors: An Introduction Including Nanophysics and Applications*, 3rd edn. (Springer, Berlin, 2016)
26. P. Ščajev, V. Gudelis, K. Jarašiūnas, I. Kisialiou, E. Ivakin, M. Nesládek, K. Haenen, Carrier recombination and diffusivity in microcrystalline CVD-grown and single-crystalline HPHT diamonds. Phys. Status Solidi A **209**, 1744 (2012)
27. A. Kanevce, M.O. Reese, T.M. Barnes, S.A. Jensen, W.K. Metzger, The roles of carrier concentration and interface, bulk, and grain-boundary recombination for 25% efficient CdTe solar cells. J. Appl. Phys. **121**, 214506 (2017)
28. D.P. Joshi, D.P. Bhatt, Theory of Grain Boundary Recombination and Carrier Transport in Polycrystalline Silicon Under Optical Illumination. IEEE Trans. Electron. Dev. **31**, 237 (1990)
29. L. Subačius, K. Jarašiūnas, P. Ščajev, M. Kato, Development of a microwave photoconductance measurement technique for the study of carrier dynamics in highly-excited 4H-SiC. Meas. Sci. Technol. **26**, 125014 (2015)
30. S. Rasool, K. Saritha, K.T. Ramakrishna Reddy, L. Bychto, A. Patryn, M. Maliński, M.S. Tivanov, V.F. Gremenok, Optoelectronic properties of In_2S_3 thin films measured using surface photovoltage spectroscopy. Mater. Res. Express **6**, 076417 (2019)
31. A.R. Warrier, R. Jayakrishnan, T.T. John, C.S. Kartha, K.P. Vijayakumar, Study on optical, electronic and thermal properties of β-In_2S_3 thin films using photothermal beam deflection technique. J. Mater. Sci.: Mater. Electron. **27**, 3628 (2016)
32. P. Ščajev, A. Usikov, V. Soukhoveev, R. Aleksiejūnas, K. Jarašiūnas, Diffusion-limited nonradiative recombination at extended defects in hydride vapor phase epitaxy GaN layers. Appl. Phys. Lett. **98**, 202105 (2011)
33. V. Grivickas, J. Linnros, Carrier lifetime: free carrier absorption, photoconductivity and photoluminescence, in *Characterization of Materials*, 1st edn., ed. by E.N. Kaufmann (Wiley, Hoboken, 2012), p. 658
34. P. Ščajev, S. Miasojedovas, A. Mekys, D. Kuciauskas, K.G. Lynn, S.K. Swain, K. Jarašiūnas, Excitation-dependent carrier lifetime and diffusion length in bulk CdTe determined by time-resolved optical pump-probe techniques. J. Appl. Phys. **123**, 025704 (2018)
35. P. Ščajev, V. Gudelis, K. Jarašiūnas, P.B. Klein, Fast and slow carrier recombination transients in highly excited 4H-and 3C-SiC crystals at room temperature. J. Appl. Phys. **108**, 023705 (2010)